RSC Advances

PAPER

View Article Online
View Journal | View Issue

Cite this: *RSC Adv.*, 2020, **10**, 27805

Adsorption performance of M-doped (M = Ti and Cr) gallium nitride nanosheets towards SO_2 and NO_2: a DFT-D calculation

Hossein Roohi * and Nastaran Askari Ardehjani

The structure, adsorption characteristics, electronic properties, and charge transfer of SO_2 and NO_2 molecules on metal-doped gallium nitride nanosheets (**M-GaNNSs**; M = Ti and Cr) were scrutinized at the Grimme-corrected PBE/double numerical plus polarization (DNP) level of theory. Two types, M_{Ga}-**GaNNSs** and M_N-**GaNNSs**, of doped nanostructures were found. The M_{Ga} sites are more stable than the M_N sites. The results showed that adsorption of SO_2 and NO_2 molecules on $Ti_{Ga,N}$-**GaNNSs** is energetically more favorable than the corresponding $Cr_{Ga,N}$-**GaNNSs**. The stability order of complexes is energetically predicted to be as NO_2–Ti_{Ga}-**GaNNS** > NO_2–Ti_N-**GaNNS** > SO_2–Ti_{Ga}-**GaNNS** > NO_2–Cr_N-**GaNNS** > SO_2–Ti_N-**GaNNS** > NO_2–Cr_{Ga}-**GaNNS** > SO_2–Cr_N-**GaNNS** > SO_2–Cr_{Ga}-**GaNNS**. The electron population analysis shows that charge is transferred from $M_{Ga,N}$-**GaNNSs** to the adsorbed gases. The Ti_{Ga}-**GaNNS** is more sensitive than the other doped nanostructures to NO_2 and SO_2 gases. It is estimated that the sensitivity of Ti_{Ga}-**GaNNS** to NO_2 gas is more than to SO_2 gas.

Received 11th April 2020
Accepted 6th July 2020

DOI: 10.1039/d0ra03251d

rsc.li/rsc-advances

1. Introduction

At present, air pollution is a significant factor limiting economic progression.[1] The emission of toxicant gases into the air is a serious matter due to the dangers of these air pollutants.[2] The source of air pollutants might be extensive in the Earth's environment.[3] Sulfur dioxide (SO_2) and nitrogen dioxide (NO_2) are noteworthy gaseous pollutants, discharged from natural and industrial procedures which have major environmental effects.[4–6] Thus, specific harmful gas detecting will be a major advantage to daily life for all people.[7–9]

For the first time in 2005, boron nitride (BN) nanosheets were forecast.[10] The honeycomb samples of BN sheets have analogies similar to graphene with equal numbers of alternating boron and nitrogen atoms that exhibit remarkable properties.[11] The electronic properties of BN sheets can be modified by B or N vacancies, Stone–Wales defects and doping heteroatoms.[12–16] In recent years, different studies have been done *via* surface quantum engineering of BN nanosheets.[17,18] For BN modification, the doped BN nanosheets were explored for developing a sensor for detecting harmful gases.[19–21]

Recently, III–V nanostructures have attracted great attention for their potential applications in novel electronic,[22–24] optical,[25–27] and electrochemical devices.[28–30] One of the III–V nanostructures were gallium nitride nanosheets (**GaNNSs**) which have been theoretically predicted[31–33] and then experimentally discovered.[34,35] It was found that the **GaNNSs** have many remarkable properties such as a high surface area to volume ratio, high thermal stability and a tunable band gap indicating that **GaNNSs** have advantages in electronic usage such as effective gas sensor applications and so on.[36] There are some experimental studies focusing on the GaN based NO_2 and SO_2 sensors.[37–40] Bishop *et al.*[41] suggested a double Schottky junction NO_2 gas sensor based on BGaN/GaN. Triet *et al.* synthesized $Al_{0.27}Ga_{0.73}N$/GaN-based Schottky diode sensors for SO_2 gas detection.[42] For example, the adsorption capabilities of gallium nitride nanosheets towards noxious gases (such as HCN, NH_3, H_2S, H_2, CO_2 and H_2O) have been described.[43] Therefore, most of the research studies have focused on nanomaterials for increasing the adsorption of adsorbates on **GaNNSs**. For this purpose, the electronic properties of **GaNNS** can be modified by doping which generates more reactive adsorption sites.[44,45] Transition metals such as Ti, Cr, Fe, Ni and Zn have been theoretically explored as dopants in **GaNNSs** to increase the adsorption properties towards CO harmful gases.[46] The adsorption of H_2S, NH_3 and SO_2 molecules on pure and doped **GaNNSs** has been considered using first-principles calculations. The results show that the metal doped **GaNNSs** are more suitable for gas molecules detection compared with the pure ones.[47] The doping effect of metal atoms on the electronic properties of **GaNNSs** was studied for tuning the optoelectronic properties, gas adsorption, hydrogen storage and catalytic reaction.[48–51] The electronic and optical properties of **GaNNSs** as a function of thickness and strain with predictive calculations were scrutinized.[52] Based on the results reported about the magnetic properties of **GaNNSs**, the metallic and

Computational Quantum Chemistry Laboratory, Department of Chemistry, Faculty of Science, University of Guilan, Rasht, Iran. E-mail: hroohi@guilan.ac.ir; Fax: +98 131 3233262

ferromagnetic properties of **GaNNS**s can be attained by semi-hydrogenation.[53] The chemical oxidation of **GaNNS**s was explored by using first-principles calculations[54] that show the oxygen adsorption mechanism can be useful for application in novel semiconducting materials. So, it would be attractive to continue investigating the promising applications of **GaNNS**s in gas sensors.

To the best of our knowledge, this is the first report on the adsorption of SO_2 and NO_2 molecules on the surface of Ti and Cr doped **GaNNS**s. The influence of transition metals doping on the adsorption behavior of SO_2 and NO_2 on the metal doped **GaNNS**s for exploring the possibility of using the doped **GaNNS**s as candidates for removing and sensing of these molecules was considered herein at the Grimme-corrected PBE/double numerical plus polarization (DNP) level of theory.

2. Computational details

In this theoretical research, the double numerical plus polarization (DNP) basis sets were selected implemented in the DMol^3 package.[55,56] The periodic spin-unrestricted DFT calculation is employed using generalized-gradient approximation (GGA) with the Perdew–Burke–Ernzerhof (PBE) functional.[57] The density functional semi-core pseudopotentials (DSPP) were generated by fitting all-electron relativistic DFT results.[58]

To consider the van der Waals (vdW) interactions, an empirical dispersion-corrected density functional theory (DFT-D) was used in the calculations. The Brillouin zone integration was sampled using a $10 \times 10 \times 1$ Monkhorst–Pack grid. A convergence tolerance of energy of 1.0×10^{-5} Ha, maximum force of 0.001 Ha per Å and maximum displacement of 0.005 Å were employed in all the geometry optimizations. To get reliable results, the real space global orbital cutoff radius was set as high as 5.2 Å and the smearing of electronic occupations to be 0.005 Ha.

To calculate the adsorption energies (AE) of the SO_2 and NO_2 molecules on the pure and metal doped **GaNNS**s, the following equation is given:

$$AE = E_T - [E_S + E_m] \quad (1)$$

where E_T, E_S and E_m are the energies of gas–**M-GaNNS**s complexes, **M-GaNNS**s and SO_2 or NO_2 molecules, respectively.

3. Results and discussion

3.1. Adsorption of SO_2 and NO_2 gas molecules over pure GaNNSs

The optimized geometries of adsorbed molecules and gallium nitride nanosheets are displayed in Fig. 1. As demonstrated in Fig. 1, the calculated bond lengths of X=O (X = N and S) in free SO_2 and NO_2 molecules are 1.482 Å and 1.201 Å, respectively, and that of the Ga–N bond length in the optimized geometry of **GaNNS** is 1.861 Å.

To find the most stable complexes obtained from adsorption of SO_2 and NO_2 gas molecules on the **GaNNS**, several configurations of SO_2 and NO_2 molecules on top of the GaNNSs are explored. The most stable adsorption complexes are illustrated in Fig. 1. After optimization, the C_2 axis of the SO_2 molecule is parallel to the **GaNNS** and that of the NO_2 molecule is perpendicular to the nanosheet. As presented in Table 1, the nearest distances between the SO_2 and NO_2 molecules with **SO_2–GaNNS** and **NO_2–GaNNS** are 1.782 Å and 2.298 Å, respectively.

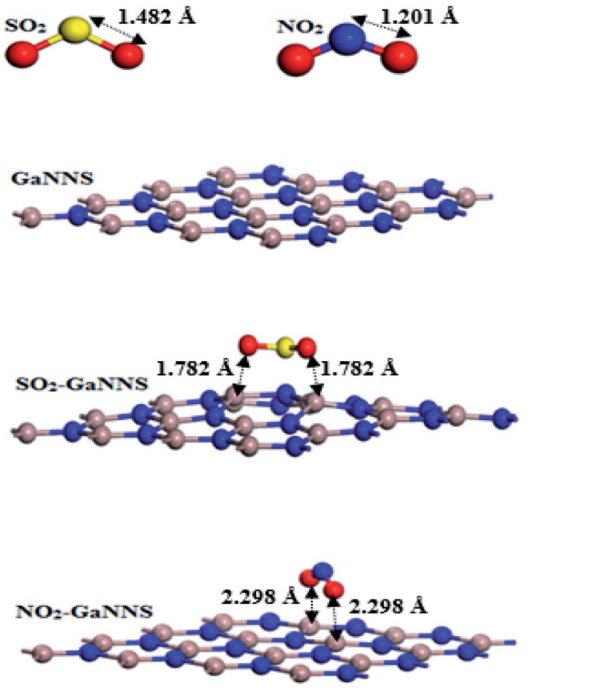

Fig. 1 The optimized geometries of SO_2, NO_2, pure and most stable adsorption complexes of **GaNNS**s.

The values of the adsorption energies (AEs) are −27.22 and −11.86 kcal mol^{-1} for **SO_2–GaNNS** and **NO_2–GaNNS** complexes, in good agreement with the smaller **SO_2–GaNNS** distance obtained. Hence, the SO_2 and NO_2 molecules are chemically adsorbed on the **GaNNS**s. The adsorption energy for the SO_2 molecule on the **GaNNS** is comparable with those found for graphene (−6.45 kcal mol^{-1})[59] and boron nitride nanosheet (−7.14 kcal mol^{-1}).[21] For adsorption of NO_2 on graphene, the calculated adsorption energy is −11.06 kcal mol^{-1}.[41]

The Hirshfeld charges on the Ga and N atoms in pristine **GaNNS** are 0.39*e* and −0.39*e*, respectively, which change to 0.40*e* and −0.38*e* in **SO_2–GaNNS**, and 0.39*e* and −0.39*e* in **NO_2–GaNNS**. The charges on S and O change from 0.38*e* and −0.19*e*

Table 1 The calculated adsorption energy (AE), equilibrium distance between molecules and nanosheet (*D*), charge of Ga and N atoms (*Q*), charge transfer (CT) and band gaps for the most stable adsorption complexes

Configurations	AE (kcal mol^{-1})	*D* (Å)	*Q* (*e*)	CT (*e*)	Band gap (eV)
Pure **GaNNS**	—	—	0.39^{Ga} $(-0.39)^{N}$	—	2.52
SO_2–GaNNS	−27.22	1.782	0.40 (−0.38)	0.17	2.51
NO_2–GaNNS	−11.86	2.298	0.39 (−0.39)	0.09	0.29

Table 2 Mulliken electron population of the total and each of the s, p and d orbitals before and after interactions

		Orbital					Orbital		
	Total pop.	s	p	d		Total pop.	s	p	d
Free SO_2					**NO_2–Cr_{Ga}-GaNNS**				
S	15.558	5.838	8.872	0.848	N	6.72	3.637	2.942	0.14
O	8.22	3.836	4.346	0.04	O	8.346	3.839	4.461	0.047
Free NO_2					Cr	13.317	2.592	6.454	4.272
N	6.646	3.449	3.028	0.17	**NO_2–Cr_N-GaNNS**				
O	8.176	3.851	4.272	0.055	N	6.759	3.684	2.951	0.124
SO_2–GaNNS					O	8.343	3.852	4.443	0.05
S	15.514	5.674	8.922	0.918	Cr	13.917	2.71	6.441	4.767
O	8.424	3.846	4.546	0.032	**SO_2–Ti_{Ga}-GaNNS**				
NO_2–GaNNS					S	15.613	5.802	9.203	0.608
N	6.669	3.541	2.972	0.156	O	8.364	3.834	4.499	0.031
O	8.25	3.841	4.36	0.049	Ti	11.018	2.433	6.304	2.281
Ti_{Ga}-GaNNS					**SO_2–Ti_N-GaNNS**				
Ti	11.244	2.658	6.202	2.384	S	15.651	5.82	9.29	0.542
Ti_N-GaNNS					O	8.384	3.832	4.522	0.03
Ti	11.465	2.612	6.347	2.505	Ti	11.322	2.51	6.383	2.43
Cr_{Ga}-GaNNS					**SO_2–Cr_{Ga}-GaNNS**				
Cr	13.357	2.655	6.345	4.357	S	15.706	5.81	9.364	0.533
Cr_N-GaNNS					O	8.399	3.837	4.531	0.03
Cr	14.014	2.888	6.232	4.894	Cr	13.286	2.589	6.463	4.234
NO_2–Ti_{Ga}-GaNNS					**SO_2–Cr_N-GaNNS**				
N	6.72	3.644	2.932	0.142	S	15.6	5.802	9.198	0.6
O	8.4	3.838	4.518	0.042	O	8.423	3.856	4.532	0.034
Ti	11.048	2.45	6.3	2.3	Cr	13.842	2.714	6.462	4.667
NO_2–Ti_N-GaNNS									
N	6.734	3.666	2.934	0.134					
O	8.382	3.86	4.478	0.046					
Ti	11.386	2.516	6.44	2.43					

in free SO_2 to 0.33 e and $-0.25e$ in **SO_2–GaNNS**, respectively. Besides, the charges on N and O are 0.17e and $-0.09e$ which change to 0.11e and $-0.10e$ in **NO_2-GaNNS**. This reveals that oxygen atoms in **SO_2–GaNNS** and **NO_2–GaNNS** complexes have the main contribution to charge transfer between the gas and nanosheet. The charge analyses show that the 0.17e and 0.09e charges are shifted from the **GaNNS**s to the SO_2 and NO_2 molecules, respectively, in good agreement with greater AE found for the **SO_2–GaNNS** complex.

The negative AEs demonstrate the orbital interactions between the gases and **GaNNS**. The Mulliken electron populations of the total and each of the s, p and d orbitals before and after interactions are given in Table 2. Inspection of the s, p and d orbital contributions in the free gases and in the **SO_2–GaNNS** and **NO_2–GaNNS** complexes indicate that the p orbital of the S atom in **SO_2–GaNNS** and O atom in **NO_2–GaNNS** have the most contribution in the interaction of molecules with the d orbital of Ga and p orbital of N atoms in the **GaNNS**. Comparison of the total electron population of orbitals shows that the population increases by 0.352e for SO_2 and 0.169e for NO_2 after interaction of the gas with the surface. This indicates that the adsorbates will get electrons from the **GaNNS**s. The change in the electronic population of the orbitals in **SO_2–GaNNS** is greater than for **NO_2–GaNNS**, in good agreement with the greater AE and Hirshfeld charge transfer values found for **SO_2–GaNNS** compared with **NO_2–GaNNS**.

3.2. Ti and Cr doped GaNNSs

In order to investigate the effect of metal doping on the geometrical and electronic properties of the **GaNNS**s, one of the central atoms in the nanosheet was substituted by Ti and Cr metal atoms. Hereafter, **M_{Ga}-GaNNS** and **M_N-GaNNS** denote that Ga and N atoms in **GaNNS** have been substituted by M metal atoms, respectively.

The optimized structures of **$M_{N(Ga)}$-GaNNS**s are illustrated in Fig. 2. The average bond distances between the metal atoms and the neighboring atoms are given in Table 3. The results show that the M–Ga bonds in **M_N-GaNNS** nanostructures are longer than the M–N bonds in **M_{Ga}-GaNNS**s. For example, the Ti–Ga and Cr–Ga bonds are longer than the Ti–N and Cr–N bonds by about 0.92 and 0.62 Å, respectively. Accordingly, it is predicted that binding of the metal to the nanosheet is stronger for **M_{Ga}-GaNNS** than **M_N-GaNNS**. Fig. 2 presents the three bond angles A_1, A_2 and A_3 around the M atoms of the NS and their average values are listed in Table 3. The averages of the three bond angles are 120.0°, 119.9°, 83.1° and 87.1° in **Ti_{Ga}-GaNNS**, **Cr_{Ga}-GaNNS**, **Ti_N-GaNNS** and **Cr_N-GaNNS**, respectively.

The binding energies (BEs) of **Ti_{Ga}-GaNNS**, **Ti_N-GaNNS**, **Cr_{Ga}-GaNNS** and **Cr_N-GaNNS** are -330.5, -236.1, -246.9 and -61.6 kcal mol^{-1}, respectively (Table 3). It is found that the BEs increase in the order **M_{Ga}-GaNNS**s > **M_N-GaNNS**s so that the value for the **Ti_{Ga}-GaNNS** structure is greater than other ones. Therefore, the Ga sites for M doping are energetically more appropriate

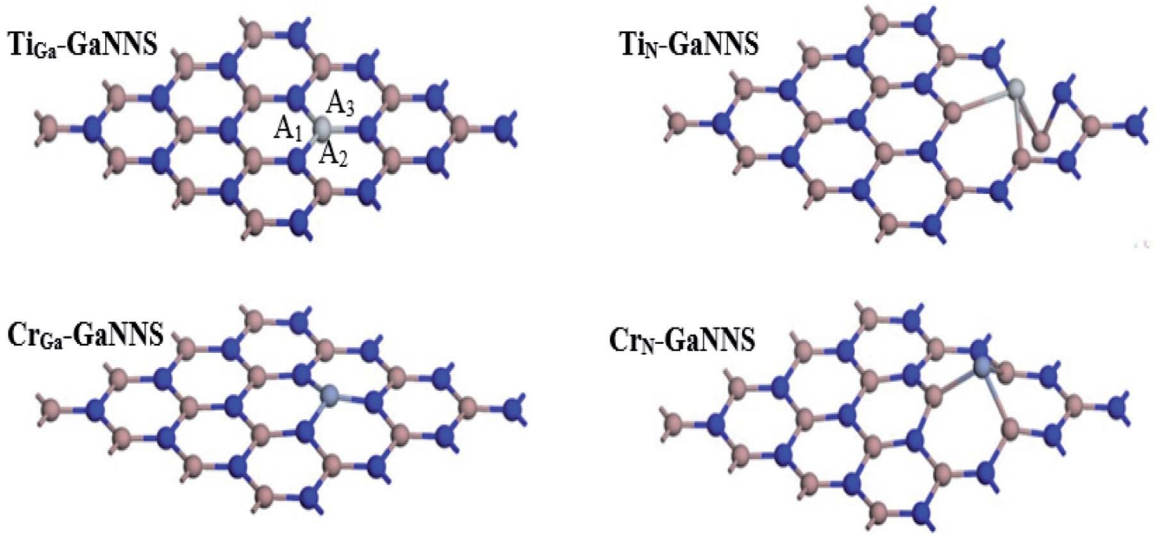

Fig. 2 Optimized geometries of Ti and Cr doped GaNNSs.

Table 3 The calculated average of M–N and M–Ga bond distances, average of bond angles (A_1, A_2 and A_3), binding energies of pristine and M (M = Ti and Cr) doped GaNNSs and Hirshfeld charge values of M atoms

Configurations	Bond distances (Å)	Bond angle (°)	Binding energies (kcal mol^{-1})	Q (e)
GaNNS	1.862	118.2	—	—
Ti$_{Ga}$-GaNNS	1.913	120.0	−330.5	0.30
Ti$_N$-GaNNS	2.838	83.1	−236.1	0.26
Cr$_{Ga}$-GaNNS	1.883	119.9	−246.9	0.43
Cr$_N$-GaNNS	2.505	87.1	−61.6	0.28

than N sites. The sequence of BEs for the **M$_{Ga}$-GaNNS** series is **Ti$_{Ga}$** > **Cr$_{Ga}$** and that of the **M$_N$-GaNNS** series is **Ti$_N$** > **Cr$_N$**. The more-negative BE indicates that the adatom is easier to be incorporated into the **GaNNS** and M doped **GaNNS**s are stable.

The Hirshfeld[44] charge values of M atoms for **M-GaNNS**s are shown in Table 3. The results show that the charge of the M atom in all M-doped **GaNNS**s is positive, indicating that the **GaNNS** in many cases acts as an electron-withdrawing support. The considerable electron transfer from the metal atom to the **GaNNS** leads to the strong bonding between the M atom and its neighbor atoms and stabilization of single-metal doped **GaNNS**. Besides, the positive charge of the M atom in **M$_{Ga}$-GaNNS**s is more than **M$_N$-GaNNS**s, in good agreement with their binding energy (BE) and the average value of the M–NS bond length. Thus, because of greater transfer of charge between the nanosheet and M atoms in **M$_{Ga}$-GaNNS**s with respect to the corresponding **M$_N$-GaNNS**s, the **M$_{Ga}$-GaNNS**s are predicted to be more stable than **M$_N$-GaNNS**s.

3.3. Adsorption of SO_2 and NO_2 gas molecules over Ti-doped GaNNSs

Now, we investigate the adsorption of SO_2 and NO_2 gas molecules on the Ti-doped **GaNNS**s as displayed in Fig. 3. Our results show that for the **SO$_2$–Ti$_{Ga}$-GaNNS** and **NO$_2$–Ti$_{Ga}$-GaNNS** complexes, the averages of the three binding distances (Ti–N) are 1.901 Å and 1.899 Å, respectively. For the **SO$_2$–Ti$_N$-GaNNS** and **NO$_2$–Ti$_N$-GaNNS** complexes, the averages of the three binding distances (Ti–Ga) are 2.983 Å and 2.949 Å, respectively. The calculated averages of the bond lengths of the S–O and N–O bonds in **SO$_2$–Ti$_{Ga}$-GaNNS**, **SO$_2$–Ti$_N$-GaNNS**, **NO$_2$–Ti$_{Ga}$-GaNNS** and **NO$_2$–Ti$_N$-GaNNS** have increased from 1.482 and 1.201 Å to 1.576, 1.606, 1.274 and 1.288 Å, respectively. These results show that the change in the SO_2 and NO_2 bond lengths upon adsorption on the **Ti$_N$-GaNNS** is greater than those of **Ti$_{Ga}$-GaNNS**.

The modified surface of Ti-doped **GaNNS**s facilitates the doped region to interact with approaching SO_2 and NO_2 molecules because of the higher chemical reactivity of the doped M atom. The results show that the $SO_2\cdots$Ti distance of **SO$_2$–Ti$_{Ga}$-GaNNS** complex is larger than **SO$_2$–Ti$_N$-GaNNS** ones. Also, the $NO_2\cdots$Ti distance for the **NO$_2$–Ti$_N$-GaNNS** complex is larger than for **NO$_2$–Ti$_{Ga}$-GaNNS**, indicating that the interaction in these complexes is stronger than in other ones.

The range of adsorption energies for SO_2 and NO_2 adsorbed on Ti-doped **GaNNS**s was between −58.36 to −61.06 and −70.68 to −76.83 kcal mol^{-1}, respectively. The negative value of the AE indicates that adsorption of SO_2 and NO_2 on Ti doped **GaNNS**s is an exothermic process. It is found that SO_2 and NO_2 molecules are adsorbed on **Ti$_N$-GaNNS**s in the sequence **NO$_2$–Ti$_N$-GaNNS** > **SO$_2$–Ti$_N$-GaNNS** and on the **Ti$_{Ga}$-GaNNS**s in the order **NO$_2$–Ti$_{Ga}$-GaNNS** > **SO$_2$–Ti$_{Ga}$-GaNNS**. Besides, it is found that the SO_2 and NO_2 adsorption energy values on **Ti$_{Ga}$-GaNNS**s are greater than on **Ti$_N$-GaNNS**s. The obtained results indicate that the adsorption capability of **Ti$_{Ga}$-GaNNS**s is greater than that of **Ti$_N$-GaNNS**s. Our results show that SO_2 and NO_2 molecules are chemically adsorbed on all **Ti$_{Ga,N}$-GaNNS**s.

The Hirshfeld population analysis presents that the charges are transferred from the **Ti$_{Ga,N}$-GaNNS**s complexes to the SO_2 and NO_2 molecules. In other words, SO_2 and NO_2 act as electron

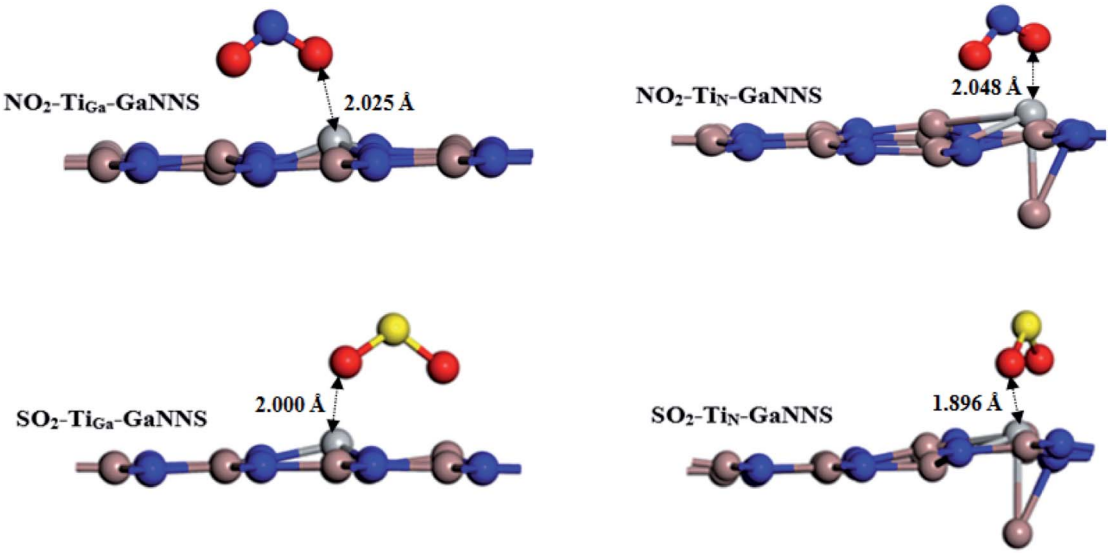

Fig. 3 The most stable adsorption configurations of SO_2 or NO_2 on Ti-doped GaNNSs.

Table 4 Adsorption energy (AE), the shortest equilibrium distance between molecules and nanosheet (D) and Hirshfeld charge transfer (CT) for the most stable configurations of SO_2 and NO_2 on metal doped GaNNSs

Configurations	AE (kcal mol^{-1})	D (Å)	CT[a] (e)
NO_2			0.00
NO_2–Ti_{Ga}-GaNNS	−76.83	2.025	0.21
NO_2–Ti_N-GaNNS	−70.68	2.048	0.25
NO_2–Cr_{Ga}-GaNNS	−54.79	1.912	0.22
NO_2–Cr_N-GaNNS	−60.81	1.952	0.31
SO_2			
SO_2–Ti_{Ga}-GaNNS	−61.06	2.000	0.16
SO_2–Ti_N-GaNNS	−58.36	1.896	0.21
SO_2–Cr_{Ga}-GaNNS	−40.46	1.834	0.27
SO_2–Cr_N-GaNNS	−53.28	2.124	0.26

[a] Absolute value of the sum of atomic charges in complexed gases.

acceptors. There is a correlation between charge transfer values and adsorption energy in the process of adsorption of SO_2 and NO_2 on the **GaNNSs**. Comparison of charge transfer values between M-doped **GaNNSs** and SO_2 and NO_2 molecules demonstrate that the value for adsorption of NO_2 is greater than that of the corresponding SO_2 one, with the exception of that obtained for **Cr_{Ga}-GaNNS**. This indicates that other parameters than charge transfer are responsible for the stability of the complexes.

The electron populations of orbitals given in Table 2 show that population of d-orbitals as well as total population of the M metals decrease upon the interaction of gases with **$Ti_{Ga,N}$-GaNNSs**. Besides, total electron population of orbitals in gases increases after adsorption of gases on the surface. This finding reveals that gases will take the electrons from **$Ti_{Ga,N}$-GaNNSs**. After adsorption of gases, total electron populations of orbitals of NO_2 (0.522e for **NO_2–Ti_{Ga}-GaNNS** and 0.500e for **NO_2–Ti_N-**

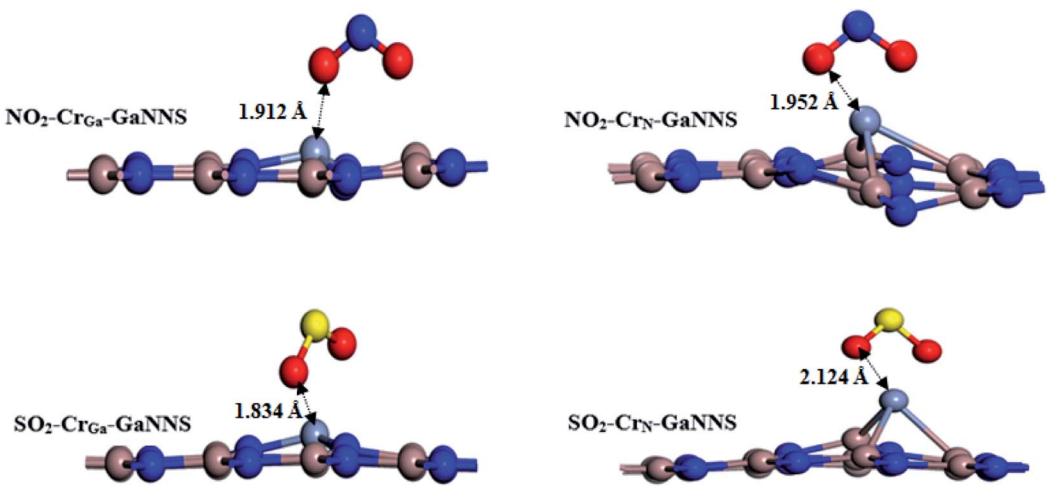

Fig. 4 The most stable adsorption configurations of SO_2 or NO_2 on Cr-doped GaNNSs.

Table 5 The E_{HOMO}, E_{LUMO}, the HOMO–LUMO gap and gap change of pure and NO_2 or SO_2 on M doped GaNNSs

Configurations	E_{HOMO} (eV)	E_{LUMO} (eV)	E_g (eV)	ΔE_g (eV)
GaNNS	−5.75	−3.23	2.52	—
Ti_{Ga}-GaNNS	−3.76	−3.28	0.47	2.05
Ti_N-GaNNS	−4.50	−3.60	0.90	1.62
Cr_{Ga}-GaNNS	−4.28	−3.64	0.64	1.88
Cr_N-GaNNS	−4.26	−3.78	0.47	2.05
NO_2–GaNNS	−5.83	−5.53	0.29	2.23
NO_2–Ti_{Ga}-GaNNS	−5.90	−3.62	2.28	1.81
NO_2–Ti_N-GaNNS	−4.96	−4.01	0.95	0.05
NO_2–Cr_{Ga}-GaNNS	−4.52	−3.87	0.65	0.01
NO_2–Cr_N-GaNNS	−5.08	−4.18	0.91	0.44
SO_2–GaNNS	−5.90	−3.37	2.11	0.41
SO_2–Ti_{Ga}-GaNNS	−4.69	−3.29	1.39	0.92
SO_2–Ti_N-GaNNS	−4.59	−3.47	1.11	0.21
SO_2–Cr_{Ga}-GaNNS	−3.45	−2.91	0.53	0.11
SO_2–Cr_N-GaNNS	−3.82	−3.53	0.28	0.19

GaNNS) are greater than those of SO_2 (0.343*e* for **SO_2–Ti_{Ga}-GaNNS** and 0.421*e* for **SO_2–Ti_N-GaNNS**), in good agreement with the greater AEs found for **NO_2–$Ti_{Ga,N}$-GaNNS** complexes. The decrease in total electron population of Ti before and after interaction is −0.196*e* and −0.079*e* in **NO_2–Ti_{Ga}-GaNNS** and **NO_2–Ti_N-GaNNS**, respectively, in good agreement with the greater AE found for **NO_2–Ti_{Ga}-GaNNS**. Besides, the total electron population of Ti after interaction with SO_2 decreases by −0.226*e* and −0.143*e* in **SO_2–Ti_{Ga}-GaNNS** and **SO_2–Ti_N-GaNNS**, respectively, in good agreement with the greater AE found for **SO_2–Ti_{Ga}-GaNNS**.

3.4. Adsorption of SO_2 and NO_2 gas molecules over Cr-doped GaNNSs

For the **SO_2–Cr_{Ga}-GaNNS** and **NO_2–Cr_{Ga}-GaNNS** complexes, the averages of three binding distances (Ti–N) are 1.834 Å and 1.912 Å, respectively. The calculated averages of bond lengths of S–O and N–O bonds in **SO_2–Cr_{Ga}-GaNNS**, **SO_2–Cr_N-GaNNS**, **NO_2–Cr_{Ga}-GaNNS** and **NO_2–Cr_N-GaNNS** have increased from 1.482 Å to 1.527, 1.574, 1.277 and 1.307 Å, respectively. For the **SO_2–Cr_N-GaNNS** and **NO_2–Cr_N-GaNNS** complexes, the averages of the three binding distances (Ti–Ga) are 2.124 Å and 1.952 Å, respectively. These results show that the change in the SO_2 and NO_2 bond lengths upon adsorption on the **Cr_N-GaNNS** is greater than that for **Cr_{Ga}-GaNNS**. The optimized structures of the NO_2 and SO_2 adsorbed on Cr-doped **GaNNS**s are illustrated in Fig. 4. The modified surface of the Cr-doped **GaNNS**s facilitates the doped region to interact with approaching SO_2 and NO_2 molecules because of the higher chemical reactivity of the doped M atom. The results show that the SO_2···Cr distance for the **SO_2–**

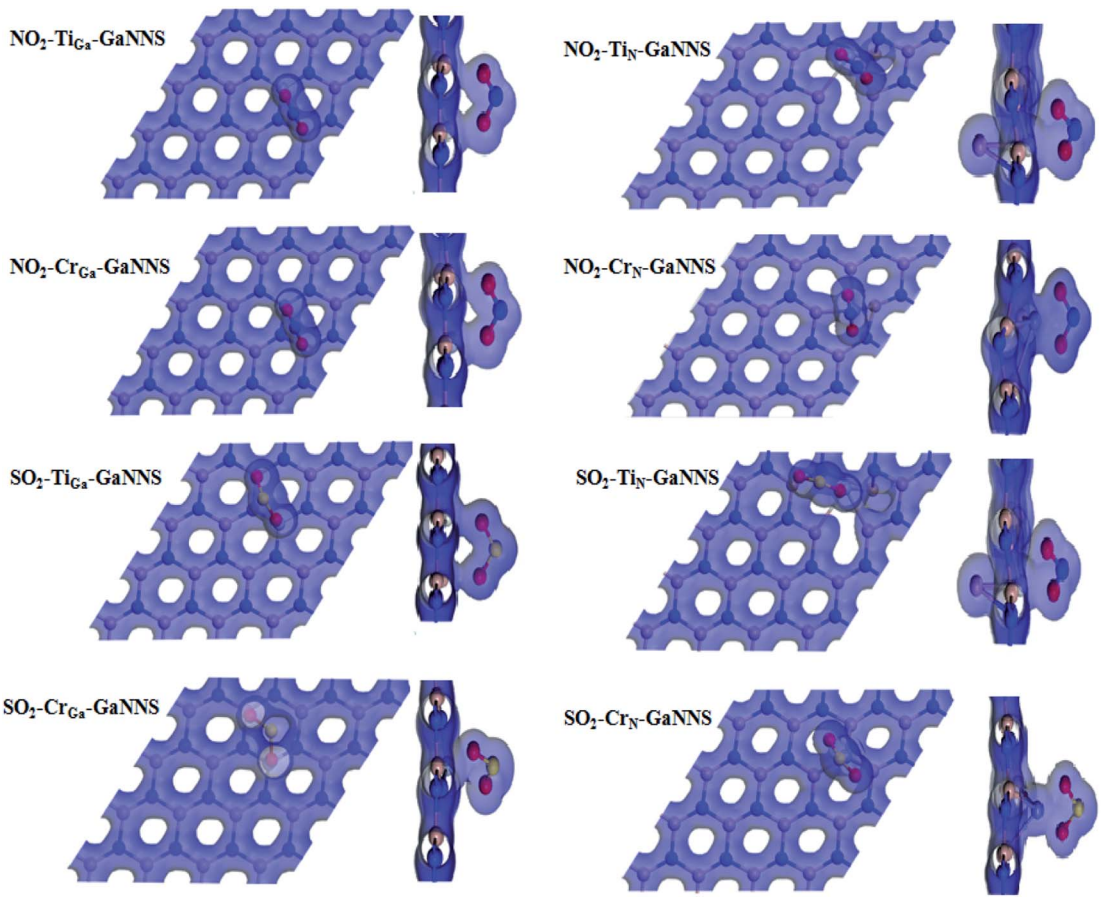

Fig. 5 The electron density schema (top and side views) of SO_2 or NO_2 adsorbed on doped GaNNSs with isovalue = 0.2*e* Å^{-3}.

Cr_N-GaNNS complex is larger than that for the **SO_2–Cr_{Ga}-GaNNS** one. Also, the $NO_2\cdots Cr$ distance for the **NO_2–Cr_N-GaNNS** complex is larger than that for **NO_2–Cr_{Ga}-GaNNS**, indicating that interaction in these complexes is stronger than for other ones.

The adsorption energies for SO_2 adsorbed on **Cr_{Ga}-GaNNS** and **Cr_N-GaNNS** are −40.46 and −53.28 kcal mol^{-1} and those for NO_2 are −54.79 and −60.81 kcal mol^{-1}, respectively. The negative value of the AE indicates that adsorption of SO_2 and NO_2 on Cr doped **GaNNS**s is an exothermic process. It is found that the ability of **Cr_N-GaNNS** towards adsorption of SO_2 and NO_2 molecules is in the sequence **NO_2–Cr_N-GaNNS** > **SO_2–Cr_N-GaNNS** and that of **Cr_{Ga}-GaNNS** is in the order **NO_2–Cr_{Ga}-GaNNS** > **SO_2–Cr_{Ga}-GaNNS**. In addition, it is found that SO_2 and NO_2 adsorption energies on **Cr_N-GaNNS** are greater than on **Cr_{Ga}-GaNNS**. The obtained results indicate that the adsorption capability of **Cr_N-GaNNS** is greater than **Cr_{Ga}-GaNNS**. Our results show that SO_2 and NO_2 molecules are chemically adsorbed on all M-doped **GaNNS**s.

The Hirshfeld population analysis shows that the charges are transferred from the **$Cr_{Ga,N}$-GaNNS** complexes to the SO_2 and NO_2 molecules. As can be seen in Table 4, the CT values are 0.22*e*, 0.31*e*, 0.27*e* and 0.26*e* in **NO_2–Cr_{Ga}-GaNNS**, **NO_2–Cr_N-GaNNS**, **SO_2–Cr_{Ga}-GaNNS** and **SO_2–Cr_N-GaNNS**, respectively. This finding reveals that the charge transferred from the nanosheet to the gas in **NO_2–Cr_N-GaNNS** is greater than in other complexes, in good agreement with the greater AE obtained for these complexes. It should be noted that other parameters than charge transfer can affect the adsorption of gases.

Analysis of the electron population of orbitals involved in the interaction between gases and nanosheets given in Table 2 reveals that the total electron population of Cr decreases by −0.040*e*, −0.097*e*, −0.071*e* and −0.172*e* in **NO_2–Cr_{Ga}-GaNNS**, **NO_2–Cr_N-GaNNS**, **SO_2–Cr_{Ga}-GaNNS**, **SO_2–Cr_N-GaNNS**, respectively, in good agreement with the greater AE found for **$NO_2(SO_2)$–Cr_N-GaNNS**s compared with **$NO_2(SO_2)$–Cr_{Ga}-GaNNS**s. In addition, the results show that the population of d-orbitals of Cr decreases and those of the NO_2 and SO_2 gases increase upon interaction with **$Cr_{Ga,N}$-GaNNS**s. This finding demonstrates that gases will get electrons from **$Cr_{Ga,N}$-GaNNS**s, in good agreement with the computed Hirshfeld charge transfer from the surface to adsorbed gases.

3.5. HOMO and LUMO based electronic properties

There is an obvious difference between the electronic properties of doped and un-doped **GaNNS**s. As can be seen in Table 5, compared to pristine **GaNNS**, the energy of the highest occupied molecule orbital (HOMO) increases and that of the lowest un-occupied molecular orbital (LUMO) decreases in doped **GaNNS** so that the amount of increase in HOMO is greater than decrease in LUMO. After adsorption of NO_2, the energies of the HOMO and LUMO decrease, but the LUMO energy shows a further decrease. In the case of SO_2, adsorption of gas on the Ti-doped **GaNNS** decreases both the HOMO and LUMO, but its adsorption on the Cr-doped **GaNNS** increases them. These changes in HOMO and LUMO energy levels lead to a change in the HOMO–LUMO gap and, in turn, in the electronic properties of **GaNNS**.

The results indicate that the band gap energies in both $M_{Ga,N}$ doped **GaNNS**s are smaller than the pure **GaNNS**, making it more conductive. The results given in Table 5 demonstrate that the band gap value of pristine **GaNNS** is 2.52 eV that changes to 2.11 eV in **SO_2–GaNNS** and 0.29 eV in **NO_2–GaNNS**. Because of the greater decrease in the LUMO level in **NO_2–GaNNS** with respect to that of **SO_2–GaNNS**, the change in the band gap for **SO_2–GaNNS** is lesser than for **NO_2–GaNNS**. Therefore, it is predicted that **GaNNS** is more sensitive to NO_2 gas than SO_2 gas. So, the large changes in band gap value for **GaNNS** (2.52 to 0.29 eV) with NO_2 gas molecule adsorption can lead to a significant change in electrical conductivity.

The electronic properties of doped **GaNNS**s are affected by the adsorption of SO_2 and NO_2 molecules. Upon adsorption of SO_2 and NO_2 molecules on the **$Ti_{Ga,N}$-GaNNS** complexes the energy gap decreases in comparison with the pristine **GaNNS**. The energy gap values are in the sequences **SO_2–Ti_N-GaNNS** (1.11 eV) > **NO_2–Ti_N-GaNNS** (0.95 eV) and **NO_2–Ti_{Ga}-GaNNS** (2.28 eV) > **SO_2–Ti_{Ga}-GaNNS** (1.39 eV). Reduction of the band gap for **SO_2–Ti_N-GaNNS** is more than for **NO_2–Ti_N-GaNNS** and that for **NO_2–Ti_{Ga}-GaNNS** is more than for **SO_2–Ti_{Ga}-GaNNS**. Therefore, it can be concluded that the sensitivity of **Ti_N-GaNNS** to SO_2 gas

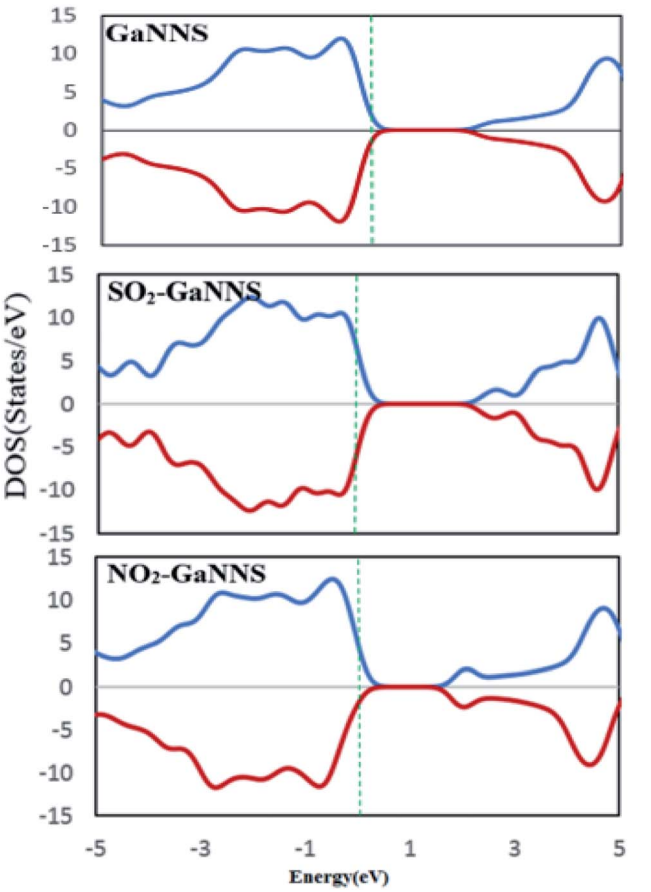

Fig. 6 The densities of states (DOSs) of GaNNS and SO_2 (NO_2) adsorbed on pristine GaNNSs.

is greater than to NO_2 gas. Besides, for **Ti_{Ga}-GaNNS**, it is predicted that the sensitivity to NO_2 gas is more than to SO_2 gas. It is a well-known issue that reduction of the energy gap enhances the electrical conductivity. Thus, the electrical conductivities are predicted to be in the order **SO_2–Ti_N-GaNNS** > **NO_2–Ti_N-GaNNS** and **NO_2–Ti_{Ga}-GaNNS** > **SO_2–Ti_{Ga}-GaNNS**.

Also, after adsorption of SO_2 and NO_2 molecules on the **$Cr_{Ga,N}$-GaNNS** complexes the band gap decreases in comparison with the pristine **GaNNS**. The band gap values are in sequence **NO_2–Cr_N-GaNNS** (0.91 eV) > **SO_2–Cr_N-GaNNS** (0.28 eV) and **NO_2–Cr_{Ga}-GaNNS** (0.65 eV) > **SO_2–Cr_{Ga}-GaNNS** (0.53 eV). The reduction in band gap for **SO_2–Cr_{Ga}-GaNNS** is more than for **NO_2–Cr_{Ga}-GaNNS** and that for **NO_2–Cr_N-GaNNS** is more than for **SO_2–Cr_N-GaNNS**. In consequence, the conductivities of **SO_2–Cr_{Ga}-GaNNS** and **NO_2–Cr_N-GaNNS** are greater than **NO_2–Cr_{Ga}-GaNNS** and **SO_2–Cr_N-GaNNS**, respectively. Also, from the changes in band gap energy values, it is forecast that the sensitivity of **Cr_N-GaNNS** to NO_2 gas is more than to SO_2 gas.

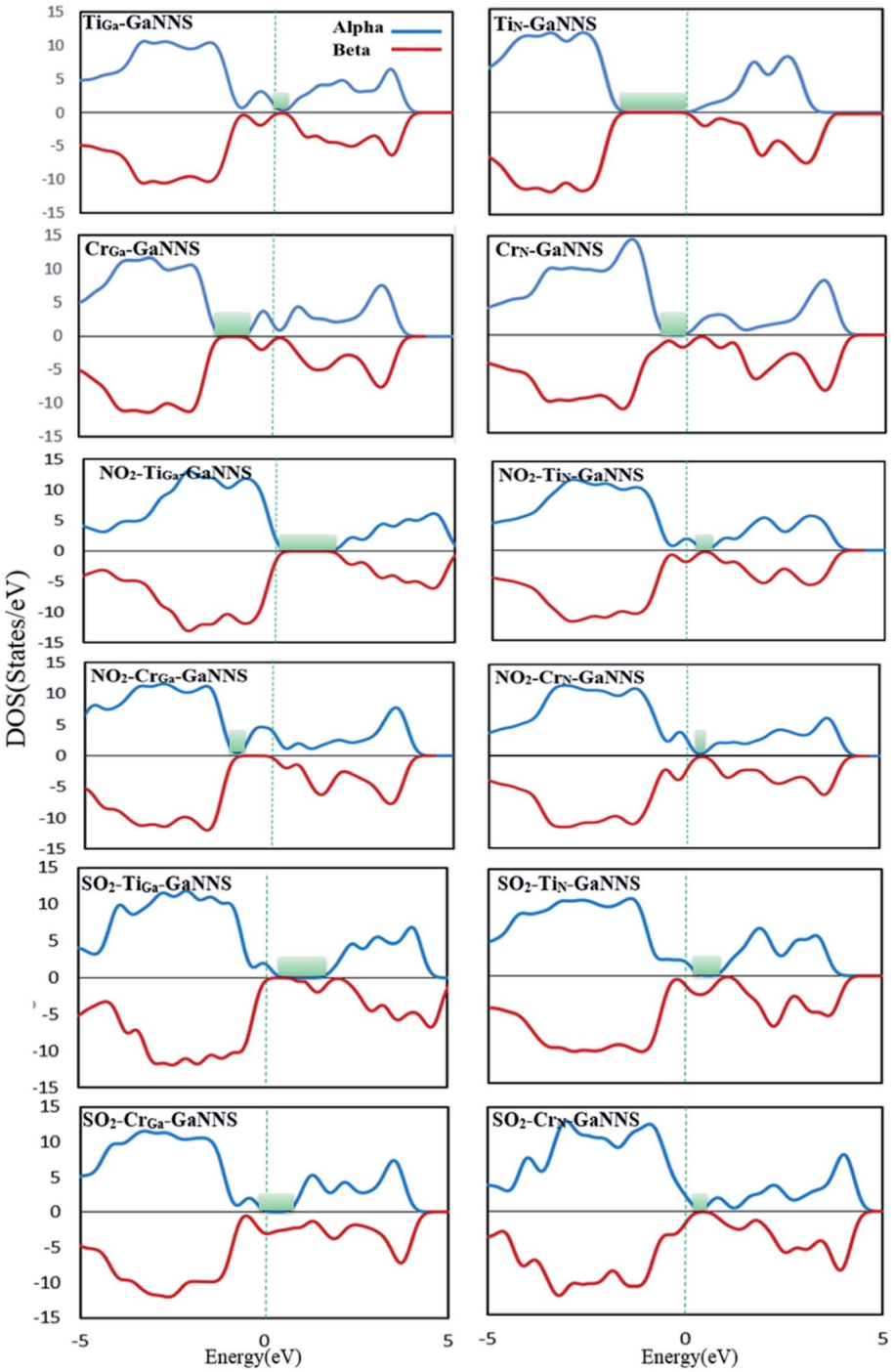

Fig. 7 The densities of states (DOSs) of SO_2 or NO_2 adsorbed on doped GaNNSs.

The top and side view plots of the electron density are illustrated in Fig. 5. An orbital overlap can be observed between the NO_2 (SO_2) gas molecules and the GaN sheets, revealing the occurrence of a strong chemisorption. It is clearly displayed that the electrons dominantly accumulate in the region between gases and **M-GaNNS**s. These results are in accordance with the obtained adsorption energies and binding distances. The orbital mixing and the charge transfer are expected to bring significant changes to the electronic structure of the GaN nanosheets which is beneficial for sensing applications. The isovalue for adsorption of gas molecules on **GaNNS** is $0.2e$ Å^{-3}.

To obtain a better understanding about the electronic properties of the complexes, densities of states (DOSs) of the nanostructures are calculated and visualized in Fig. 6 and 7. As can be observed, the **GaNNS**, **NO_2–GaNNS**, **SO_2–GaNNS**, **NO_2–Ti_{Ga}-GaNNS**, **NO_2–Ti_N-GaNNS** and **NO_2–Cr_N-GaNNS** nanostructures are nonmagnetic systems because the spin-up and spin-down in the DOS plots are the same as each other. From this figure, it can be found that new states appear in the band gap regions of **NO_2–Cr_{Ga}-GaNNS**, **SO_2–Ti_{Ga}-GaNNS**, **SO_2–Ti_N-GaNNS**, **SO_2–Cr_{Ga}-GaNNS** and **SO_2–CrN-GaNNS**. Since the spin-up and spin-down DOSs are different, **NO_2–Cr_{Ga}-GaNNS**, **SO_2–Ti_{Ga}-GaNNS**, **SO_2–Ti_N-GaNNS**, **SO_2–Cr_{Ga}-GaNNS** and **SO_2–Cr_N-GaNNS** have magnetic properties.

4. Conclusions

DFT calculations are performed to consider the adsorption of sulfur dioxide and nitrogen dioxide molecules on metal-doped gallium nitride nanosheets. The results present that adsorption of NO_2 on **M_N-GaNNS** and **M_{Ga}-GaNNS** is energetically more favorable than that of SO_2 on corresponding NSs. A brief comparison of AEs of SO_2 and NO_2 molecules on Ti and Cr doped **GaNNS**s indicates that the AEs of NO_2 and SO_2 on **$Ti_{Ga,N}$-GaNNS**s are greater than on **$Cr_{Ga,N}$-GaNNS**s. The electron populations of orbitals were calculated before and after interaction. There is a correlation between the change in electron population of orbitals of adsorbate and adsorbent and the AE obtained for complexes. The electron population analysis shows that charge is transferred from **$M_{Ga,N}$-GaNNS**s to the adsorbed gases. After the adsorption of SO_2 and NO_2 molecules, the electronic properties of the pure and doped **GaNNS**s indicate the considerable changes in the conductivity of the nanosheets. Furthermore, the sensitivity of **Ti_{Ga}-GaNNS** is predicted to be more than for other NSs toward SO_2 gas. It is estimated that the sensitivity of **Ti_{Ga}-GaNNS** to NO_2 gas is more than to SO_2 gas. Therefore, these results show that **GaNNS**-based materials can be used as noxious gas sensors.

Conflicts of interest

The all authors declare that they have no conflict of interest.

Acknowledgements

This work was supported by the University of Guilan and Iran National Science Foundation through research facilities and financial grants.

References

1 Y. Zhang, S. Yuan, X. Feng, H. Li, J. Zhou and B. Wang, *J. Am. Chem. Soc.*, 2016, **138**, 5785–5788.
2 A. Tiwary and I. Williams, *Air pollution: measurement, modelling and mitigation*, CRC Press, 2018.
3 V. Ramanathan and Y. Feng, *Atmos. Environ.*, 2009, **43**, 37–50.
4 R. S. Scorer, *Pollution in the air: problems, policies and priorities*, Routledge, 2019.
5 J. A. Bernstein, N. Alexis, C. Barnes, I. L. Bernstein, A. Nel, D. Peden, D. Diaz-Sanchez, S. M. Tarlo and P. B. Williams, *J. Allergy Clin. Immunol.*, 2004, **114**, 1116–1123.
6 R. Bascom, P. A. Bromberg, D. L. Costa, R. Devlin, D. W. Dockery, M. W. Frampton, W. Lambert, J. M. Samet, F. E. Speizer and M. Utell, *Am. J. Respir. Crit. Care Med.*, 1996, **153**, 477–498.
7 P. M. Mannucci, S. Harari, I. Martinelli and M. Franchini, *Intern. Emerg. Med.*, 2015, **10**, 657–662.
8 L. B. Lave and E. P. Seskin, *Air pollution and human health*, Routledge, 2013, vol. 6.
9 M. Kampa and E. Castanas, *Environ. Pollut.*, 2008, **151**, 362–367.
10 K. S. Novoselov, D. Jiang, F. Schedin, T. J. Booth, V. V Khotkevich, S. V Morozov and A. K. Geim, *Proc. Natl. Acad. Sci. U. S. A.*, 2005, **102**, 10451–10453.
11 L. H. Li and Y. Chen, *Adv. Funct. Mater.*, 2016, **26**, 2594–2608.
12 Q. Zeng, H. Wang, W. Fu, Y. Gong, W. Zhou, P. M. Ajayan, J. Lou and Z. Liu, *Small*, 2015, **11**, 1868–1884.
13 R. Ansari, S. Malakpour and S. Ajori, *Superlattices Microstruct.*, 2014, **72**, 230–237.
14 A. Bhattacharya, S. Bhattacharya and G. P. Das, *Phys. Rev. B: Condens. Matter Mater. Phys.*, 2012, **85**, 35415.
15 S. Lin, X. Ye, R. S. Johnson and H. Guo, *J. Phys. Chem. C*, 2013, **117**, 17319–17326.
16 X. Gao, S. Wang and S. Lin, *ACS Appl. Mater. Interfaces*, 2016, **8**, 24238–24247.
17 Q. Tang, Z. Zhou and Z. Chen, *J. Phys. Chem. C*, 2011, **115**, 18531–18537.
18 P. Thangasamy, M. Santhanam and M. Sathish, *ACS Appl. Mater. Interfaces*, 2016, **8**, 18647–18651.
19 M. Samadizadeh, A. A. Peyghan and S. F. Rastegar, *Chin. Chem. Lett.*, 2015, **26**, 1042–1045.
20 M. D. Esrafili and F. A. Rad, *Vacuum*, 2019, **166**, 127–134.
21 F. Behmagham, E. Vessally, B. Massoumi, A. Hosseinian and L. Edjlali, *Superlattices Microstruct.*, 2016, **100**, 350–357.
22 A. A. Tonkikh, E. N. Voloshina, P. Werner, H. Blumtritt, B. Senkovskiy, G. Güntherodt, S. S. P. Parkin and Y. S. Dedkov, *Sci. Rep.*, 2016, **6**, 23547.
23 N. Izyumskaya, D. O. Demchenko, S. Das, Ü. Özgür, V. Avrutin and H. Morkoç, *Adv. Electron. Mater.*, 2017, **3**, 1600485.

24 G. B. Pinhal, N. L. Marana, G. S. L. Fabris and J. R. Sambrano, *Theor. Chem. Acc.*, 2019, **138**, 31.
25 H. Vovusha and B. Sanyal, *RSC Adv.*, 2015, **5**, 4599–4608.
26 B. A. Ravan and H. Jafari, *Comput. Condens. Matter*, 2019, e00416.
27 K. Wang, Q. Xiao, Q. Xie, L. Wang, T. He, H. Chen and J. Shi, *J. Electron. Mater.*, 2019, **48**, 5135–5142.
28 S. Y. F. Zhao, G. A. Elbaz, D. K. Bediako, C. Yu, D. K. Efetov, Y. Guo, J. Ravichandran, K.-A. Min, S. Hong, T. Taniguchi, K. Watanabe, L. E. Brus, X. Roy and P. Kim, *Nano Lett.*, 2018, **18**, 460–466.
29 T. Ouyang, Z. Qian, R. Ahuja and X. Liu, *Appl. Surf. Sci.*, 2018, **439**, 196–201.
30 A. Sengupta, *Appl. Surf. Sci.*, 2018, **451**, 141–147.
31 A. K. Singh and R. G. Hennig, *Appl. Phys. Lett.*, 2014, **105**, 51604.
32 A. K. Singh, H. L. Zhuang and R. G. Hennig, *Phys. Rev. B: Condens. Matter Mater. Phys.*, 2014, **89**, 245431.
33 H. Zhang, F.-S. Meng and Y.-B. Wu, *Solid State Commun.*, 2017, **250**, 18–22.
34 Z. Y. Al Balushi, K. Wang, R. K. Ghosh, R. A. Vilá, S. M. Eichfeld, J. D. Caldwell, X. Qin, Y.-C. Lin, P. A. DeSario and G. Stone, *Nat. Mater.*, 2016, **15**, 1166.
35 N. A. Koratkar, *Nat. Mater.*, 2016, **15**, 1153.
36 Y. Yong, X. Su, H. Cui, Q. Zhou, Y. Kuang and X. Li, *ACS Omega*, 2017, **2**(12), 8888–8895.
37 M. Lim, S. Mills, B. Lee and V. Misra, *ECS J. Solid State Sci. Technol.*, 2015, **4**, S3034–S3037.
38 Y. Halfaya, C. Bishop, A. Soltani, S. Sundaram, V. Aubry, P. L. Voss, J.-P. Salvestrini and A. Ougazzaden, *Sensors*, 2016, **16**, 273.
39 M. A. H. Khan, B. Thomson, R. Debnath, A. Rani, A. Motayed and M. V Rao, *Nanotechnology*, 2020, **31**, 155504.
40 C. Bishop, Y. Halfaya, A. Soltani, S. Sundaram, X. Li, J. Streque, Y. El Gmili, P. L. Voss, J. P. Salvestrini and A. Ougazzaden, *IEEE Sens. J.*, 2016, **16**, 6828–6838.
41 C. Bishop, J.-P. Salvestrini, Y. Halfaya, S. Sundaram, Y. El Gmili, L. Pradere, J. Y. Marteau, M. B. Assouar, P. L. Voss and A. Ougazzaden, *Appl. Phys. Lett.*, 2015, **106**, 243504.
42 N. Minh Triet, L. Thai Duy, B.-U. Hwang, A. Hanif, S. Siddiqui, K.-H. Park, C.-Y. Cho and N.-E. Lee, *ACS Appl. Mater. Interfaces*, 2017, **9**, 30722–30732.
43 Y. Yong, H. Cui, Q. Zhou and X. Su, *RSC Adv.*, 2017, **7**, 51027–51035.
44 M. Xiao, T. Yao, Z. Ao, P. Wei, D. Wang and H. Song, *Phys. Chem. Chem. Phys.*, 2015, **17**, 8692–8698.
45 G. Chen, D. Wang, J. Wen, A. Yang and J. Zhang, *Int. J. Quantum Chem.*, 2016, **116**, 1000–1005.
46 H. Roohi and N. Askari Ardehjani, *New J. Chem.*, 2019, **43**, 15280–15292.
47 G.-X. Chen, H.-F. Li, D.-D. Wang, S.-Q. Li, X.-B. Fan and J.-M. Zhang, *Vacuum*, 2019, **165**, 35–45.
48 V. Sharma and S. Srivastava, *Mater. Res. Express*, 2018, **5**, 45001.
49 B. Sarkar, P. Reddy, A. Klump, F. Kaess, R. Rounds, R. Kirste, S. Mita, E. Kohn, R. Collazo and Z. Sitar, *J. Electron. Mater.*, 2018, **47**, 305–311.
50 M. Zhang, T. F. Zhou, Y. M. Zhang, W. Y. Wang, W. Li, Y. Bai, K. Lian, J. F. Wang and K. Xu, *J. Phys. D: Appl. Phys.*, 2018, **51**, 65105.
51 M. A. Reshchikov, P. Ghimire and D. O. Demchenko, *Phys. Rev. B*, 2018, **97**, 205204.
52 N. Sanders, D. Bayerl, G. Shi, K. A. Mengle and E. Kioupakis, *Nano Lett.*, 2017, **17**(12), 7345–7349.
53 W. Xiao, L. Wang, L. Xu, Q. Wan, A. Pan and H. Deng, *Phys. Status Solidi*, 2011, **248**, 1442–1445.
54 J. Chen, J. Zhu, J. Ning, X. Duan, D. Wang, J. Zhang and Y. Hao, *Phys. Chem. Chem. Phys.*, 2019, **21**, 6224–6228.
55 B. Delley, *J. Chem. Phys.*, 1990, **92**, 508–517.
56 D. R. Hamann, M. Schlüter and C. Chiang, *Phys. Rev. Lett.*, 1979, **43**, 1494.
57 J. P. Perdew, K. Burke and M. Ernzerhof, *Phys. Rev. Lett.*, 1996, **77**, 3865.
58 B. Delley, *Phys. Rev. B: Condens. Matter Mater. Phys.*, 2002, **66**, 155125.
59 D. Cortes-Arriagada, N. Villegas-Escobar and D. E. Ortega, *Appl. Surf. Sci.*, 2018, **427**, 227–236.

